Research Square

Preprints are preliminary reports that have not undergone peer review.
They should not be considered conclusive, used to inform clinical practice,
or referenced by the media as validated information.

Mitogenomic characterization and phylogenetic placement of the Mottled Wood-owl Strix ocellata with gene rearrangement patterns in Strigiformes

Amitava Majumder
Zoological Survey of India
Angkasa Putra
Pukyong National University
Anindya Naskar
Zoological Survey of India
Agus Mohammad Hikam
Pukyong National University
Dhriti Banerjee
Zoological Survey of India
Hyun-Woo Kim
Pukyong National University
Shantanu Kundu
shantanu1984@gmail.com

Pukyong National University

Article

Keywords: Mitochondrial DNA, Avian lineage, Nocturnal raptor, Codon usage, Phylogeny, Gene rearrangement

Posted Date: June 29th, 2026

DOI: https://doi.org/10.21203/rs.3.rs-9724069/v1

License: This work is licensed under a Creative Commons Attribution 4.0 International License. Read Full License

Additional Declarations: No competing interests reported.

Version of Record: A version of this preprint was published at Scientific Reports on September 17th, 2026. See the published version at https://doi.org/10.1038/s41598-026-71868-6.

Abstract

Owls (order Strigiformes) represent a highly specialized lineage of nocturnal raptors, within which the genus *Strix* (family Strigidae) comprises several widely distributed species despite the limited availability of comprehensive mitogenomic data. In this study, the complete mitogenome of the Mottled Wood-owl, *Strix ocellata* (Lesson, 1839), was characterized to investigate its genomic organization, structural features, and patterns of gene rearrangement. Furthermore, the phylogenetic position of *S. ocellata* was evaluated within the broader lineage of Strigiformes using concatenated mitochondrial protein-coding genes (PCGs), and among congeners using partial COI and Cytb genes. The circular mitogenome of *S. ocellata* was 19,135 bp in length and comprised the typical vertebrate mitochondrial complement of 13 PCGs, 22 transfer RNA genes (tRNAs), two ribosomal RNA genes (rRNAs), and two non-coding control regions (CRs). The selective pressure analyses revealed strong purifying selection acting across all PCGs, whereas codon usage analysis demonstrated biased synonymous codon preferences, with arginine, leucine, and serine representing the most abundant amino acids. The CR retained the three characteristic conserved domains, while variation in tandem repeat motifs suggested evolutionary divergence among the examined taxa. The phylogenetic inference based on complete mitogenome datasets strongly supported the monophyly of the genus *Strix*, although the family Strigidae appeared non-monophyletic. Notably, *S. ocellata* occupied a putatively basal position relative to other *Strix* species based on both complete mitogenomes and partial mitochondrial markers. The comparative examination of mitochondrial gene arrangements revealed a largely conserved genomic architecture across Strigiformes, with observed transposition and duplication events involving ND6, Cytb, several tRNA genes, and the CRs. Collectively, this study provides the first mitogenomic characterization of *S. ocellata* as well as evolutionary relationships within *Strix* and the broader Strigiformes lineage. Nevertheless, the current mitogenomic dataset represents only ~ 13% of the recognized Strigiformes diversity and includes merely six *Strix* species. In contrast, the partial-gene datasets encompass approximately 50–55% of recognized *Strix* species for the COI and Cytb markers, thereby providing broader taxonomic representation. These findings underscore the urgent need for additional complete mitogenome sequences to improve phylogenetic resolution and facilitate a more comprehensive understanding of the matrilineal evolutionary history of this owl lineage.

1. Introduction

Birds (Class Aves; clade Telluraves) represent one of the most species-rich vertebrate lineages, exhibiting remarkable ecological adaptability that has enabled their distribution across all terrestrial ecosystems worldwide[1,2]. Their extensive morphological diversity, behavioral complexity, and well-documented evolutionary history make birds a fundamental model for studying adaptation, speciation, biogeography, and evolutionary biology[3,4]. Within trophic networks, birds occupy multiple ecological roles ranging from primary consumers to highest-level predators, thereby contributing significantly to community structure and ecosystem functional stability[5]. According to the International Ornithologists' Committee (IOC) World Bird List, 11,250 bird species are currently recognized globally under 44 orders, 256 families, and 2,396 genera[6]. Among this diversity, raptors constitute a specialized functional assemblage that plays an important role in regulating prey population size through predation and demonstrate distinctive vocalization characteristics

that vary in complexity and frequency across taxonomic groups[7,8]. One of the major lineages within this assemblage is the order Strigiformes, which comprises all extant owl species and is distributed globally except in Antarctica and numerous remote oceanic islands[9,10]. Ecologically, members of this order are predominantly nocturnal predators that employ ambush-based hunting strategies and possess highly specialized sensory adaptations, featuring acute binaural hearing and enhanced low-light vision[11,12].

Taxonomically, Strigiformes is divided into two principal families, Strigidae (Typical owls) and Tytonidae (Barn owls)[6,13]. Notably, the family Strigidae is the largest and most taxonomically complex group, comprising three subfamilies viz., Striginae, Asioninae, and Surniinae[7]. This family includes 234 species distributed across 23 genera, with approximately 39% of the genera being monotypic[6]. Conversely, the Tytonidae is relatively small, incorporating two extant subfamilies, viz., Tytoninae, represented by the genus *Tyto* (18 species), and Phodilinae, reflected by the genus *Phodilus* (2 species)[6,14]. Despite their high species diversity, many owl species display largely cryptic morphology, and genetically inherited vocalization traits often provide valuable taxonomic signals[7,15]. They also hold substantial cultural importance across human civilizations and symbolize concepts of spiritual wisdom[16]. Simultaneously, increasing anthropogenic pressures, particularly habitat degradation and fragmentation, climate change, and persecution driven by negative cultural perceptions, pose serious threats to owl populations and may compromise species persistence as well as ecosystem functions[17].

Within the family Strigidae, the genus *Strix* constitutes a distinct evolutionary lineage containing 22 species with a broad biogeographic distribution across four major continents (Asia, Africa, Europe, and the Americas)[6]. One species within this genus is the large-bodied Mottled Wood-owl *Strix ocellata* (Lesson, 1839), which is mainly distributed in India and has also been recorded inthe bordering area of Nepal, although its origin and seasonal population dynamics outside India remain poorly understood and require further investigation[6,18]. Owing to its wide geographic distribution and absence of criteria meeting threatened category thresholds, this species is currently classified as ‘Least Concern’ according to the BirdLife International assessment published in the IUCN Red List of Threatened Species[18]. From an ecological perspective, *S. ocellata* is a terrestrial species exhibiting broad habitat tolerance, occurring in forestsopen woodland, urban parks, and other human-modified landscapes[18]. The species also demonstrates considerable adaptability to agroforestry environments by utilizing mango and tamarind trees as nesting sites, where nest tree availability is a key determinant of population persistence, with moderate reproductive success and a diet primarily consisting of insects and small vertebrates[19]. Further, multiple genetic studies on *Strix* species have addressed species delimitation and identification, genetic diversity, population divergence, phylogenetic relationships, and historical demography using partial mitochondrial sequences, nuclear markers, and microsatellite loci[7,20,21]. However, the molecular information is currently available for only ~ 55% of *Strix* species in the GenBank database, leaving nearly half of the species completely unrepresented, including *S. ocellata*. In addition, the comprehensive mitogenomic investigations within this genus also remain limited, with data available for only five *Strix* species (*S. aluco*, *S. leptogrammica*, *S. occidentalis*, *S. uralensis*, and *S. varia*) to date[22–25]. Hence, this limitation highlights the

need for further research to expand taxonomic coverage and improve evolutionary resolution within this lineage.

At the molecular level, the mitogenome is a compact, circular, double-stranded DNA molecule (~ 16–20 kb) composed of heavy and light strands, a structural organization conserved across vertebrates, including avian taxa[26]. It also typically consists of 13 protein-coding genes (PCGs) associated with the electron transport chain, 22 transfer RNA genes (tRNAs), two ribosomal RNA genes (rRNAs), and non-coding control region (CR) enriched in adenine and thymine that regulates replication and transcription[27]. Due to its maternal inheritance, relatively high mutation rate, and lack of recombination, the mitogenome serves as a highly informative molecular marker for species identification, evolutionary studies, phylogeography, and population dynamics[28]. The comparative analyses of mitogenomic sequence variation and genomic structure facilitate the verification of conserved regions and divergence signatures among species, the detection of selective pressure profiles, and clarification of phylogenetic relationships across multiple taxonomic levels, including birds[29]. Moreover, the examination of mitochondrial gene arrangement among species within Strigiformes is important for evaluating mitogenome structural stability and detecting potential gene rearrangement events that may serve as evolutionary signals[24,30]. Considering this framework, this study aims to (i) generate the first genetic data for species identification of *S. ocellata*; (ii) characterize and describe the complete mitogenomic architecture of *S. ocellata*; and (iii) analyze sequence variation and genomic features using a comparative approach with other *Strix* species available in GenBank. Additionally, this research is also designed to: (iv) evaluate phylogenetic relationships to elucidate the evolutionary lineage and taxonomic position of *S. ocellata* within the genus *Strix* and the broader Strigiformes lineage using complete and partial mitochondrial DNA datasets; and (v) construct and compare mitochondrial gene arrangement patterns among Strigiformes species to identify structurally conserved and gene rearrangements. Collectively, the findings of this study enhance the phylogenetic inference in owls, provide robust molecular evidence for evolutionary and biogeographic investigations, and contribute to the establishment of genetics-informed conservation strategies for this raptor species throughout its distributional range.

2. Materials and methods

2.1. Sample collection and ethics statement

A specimen of *S. ocellata* was opportunistically collected after being found road-killed within its natural distribution range in northern India (Fig. 1). The collection was undertaken during routine faunal survey and monitoring activities carried out by the Zoological Survey of India (ZSI) in Uttar Pradesh, India. Based on the observed morphological characters, including a whitish facial disc with dark concentric streaks, dark brown eyes, dull pinkish to coral-red eyelids, horn-black bill, and finely streaked reddish-brown dorsal plumage with a distinct black nuchal spot, the specimen was identified as *S. ocellata*[31]. The ventral plumage was white with golden-yellow suffusion and narrow black streaking, while the toes were pale yellowish-brown with horn-black claws, consistent with the observed diagnostic features of *S. ocellata*. No animals were harmed or intentionally collected for this study, and the specimen was photographed following collection. The

tissue samples were excised from the pectoral muscle for subsequent molecular analyses. The tissues were initially preserved in laboratory-grade absolute ethanol, followed by storage in a deep freezer at −20°C. The voucher specimen was subsequently deposited in the National Zoological Collections of the ZSI, Kolkata, India, under the unique voucher code ZSI-AM5 for long-term preservation and future reference. All procedures were approved by the host institute, ZSI, and complied with the ethical guidelines applicable to opportunistic wildlife sampling (No. 216 – 16/2024/Tech. Misc./8784). The study was conducted in accordance with the ARRIVE 2.0 guidelines for animal research (https://arriveguidelines.org/)[32]. The species distribution and collection locality of the road-killed *S. ocellata* are presented in Fig. 1.

2.2. Mitogenome sequencing via next-generation technology

Total mitochondrial DNA of *S. ocellata* was isolated in accordance with the protocol provided by the Alexgen DNA Kit (Alexius Biosciences, Ahmedabad, India)[33]. The integrity and concentration of the extracted DNA were quantified using a Qubit 4.0 fluorometer (Thermo Fisher Scientific, USA) to ensure that the material met the requirements for subsequent library construction. The library preparation and sequencing procedures were conducted at the Neuberg Center for Genomic Medicine, Neuberg Supratech Research Laboratories (NSRL), Ahmedabad, India. A paired-end sequencing library was generated with the QIAseq FX DNA Library Kit (Qiagen, Cat. No. 180479). Prior to adapter ligation, the genomic DNA was fragmented to the desired insert size using a Covaris M220 Focused Ultrasonicator (Covaris Inc., San Diego, CA, USA). The fragmented DNA was then ligated with platform-specific adapters compatible with Illumina sequencing systems. To increase the yield of libraries derived from limited DNA input, the amplification was performed using HiFi PCR Master Mix (Takara Bio Inc., Japan). The library quality, including fragment size distribution, was assessed on an Agilent TapeStation 4150 system using High Sensitivity D1000 ScreenTape. Only libraries that satisfied quality control criteria were advanced for sequencing on the Illumina NovaSeq 6000 platform (Illumina, San Diego, CA, USA), which generated high-throughput paired-end reads.

2.3. Mitogenome assembly, annotation, and submission

Around 25 million paired-end sequencing reads with high quality were utilized as input data for mitogenome construction of *S. ocellata*. The genome assembly and functional annotation were carried out using the bioinformatics platform Geneious Prime v2023.0.138[34]. To ensure the reliability of annotation, the genomic boundaries were evaluated through dual independent annotation workflows. In particular, the automated mitochondrial gene prediction was first conducted using MITOS2 implemented in the Galaxy web platform v2.1.10 (https://usegalaxy.eu) for de novo metazoan mitogenome annotation[35,36]. The complementary annotation verification was subsequently performed using MitoAnnotator accessible through the Mitofish server v2026.02 (https://mitofish.aori.u-tokyo.ac.jp/annotation/input)[37,38]. The integrity of PCGs was further assessed by inspecting predicted amino acid sequences using the NCBI Open Reading Frame (ORF) Finder (https://www.ncbi.nlm.nih.gov/orffinder) based on the vertebrate mitochondrial translation code[39]. Concurrently, both rRNA and tRNA genes projections were corroborated using annotation utilities available within the Galaxy platform v2.1.10. The finalized mitogenome sequence of *S. ocellata* was deposited in GenBank under accession number PX652377.

2.4. Structural analysis of mitogenome

The circular mitogenome of *S. ocellata* was visualized using MitoAnnotator to provide a representative genomic map and to identify gene boundaries, including strand orientation, using distinct color schemes. The comparative mitogenomic structural analysis was conducted between *S. ocellata* and five other *Strix* species (*S. aluco*, *S. leptogrammica*, *S. occidentalis*, *S. uralensis*, and *S. varia*), with sequences are available in GenBank and reported in previously published studies[22–25] (Supplementary Table S1). Specifically, the lengths of intergenic spacer regions and gene overlap areas were manually determined using Microsoft Excel v2016. The nucleotide composition across the complete mitogenome and within specific genomic segments, including PCGs, tRNAs, rRNAs, and CR, was measured based on the relative proportions of adenine (A), thymine (T), guanine (G), and cytosine (C) using the GC Content Calculator provided by VectorBuilder (https://en.vectorbuilder.com/tool/gc-content-calculator.html). The strand compositional bias was quantified using the standard skewness indices, calculated as AT-skew = (A − T) / (A + T) and GC-skew = (G − C) / (G + C), to characterize nucleotide distribution asymmetry within the mitogenome[40]. Both start and stop codon validation was performed using NCBI ORF Finder and subsequently verified using MEGA v12 to ensure accurate prediction of translational reading frames[41]. The nucleotide diversity was estimated using DnaSP v6.0 with a sliding window approach (length of 200 bp and step size of 25 bp)[42]. The transition–transversion substitution patterns were analyzed using DAMBE v7.3.32[43], while the ratio of nonsynonymous to synonymous substitutions (Ka/Ks) was also calculated using DnaSP v6.0 to assess evolutionary selective pressure. Both relative synonymous codon usage (RSCU) and amino acid composition were examined using MEGA v12.0 and subsequently validated using DnaSP v6.0 to ensure analytical accuracy. The secondary configuration of *S. ocellata* tRNA genes was predicted using ARAGORN via the Galaxy web platform v1.2.41 to confirm the formation of the typical mitochondrial cloverleaf tRNA structure[44]. The multiple sequence alignment of the CR, located between tRNA-Pro and tRNA-Phe, was executed using CLUSTAL W implemented in MEGA v12 to identify conserved and variable domains based on previously reported motif patterns[45,46]. In addition, the tandem repeat elements within the CR were detected using Tandem Repeats Finder (https://tandem.bu.edu/trf/trf.html) to elucidate repeat units and structural features of this non-coding region[47]. The CR framework analysis excluded *S. leptogrammica* due to the available nucleotide sequence was relatively short and insufficient for comprehensive comparative analysis.

2.5. Data assembly, phylogenetic framework, and genetic divergence

The cladistic construction in this study incorporated both mitogenomic data covering a broad representation of Strigiformes and partial mitochondrial markers (COI and Cytb) specifically targeted to the genus *Strix* to explicitly resolve the phylogenetic placement of *S. ocellata*. To achieve this intention, multiple datasets were compiled, including two mitogenome assemblies comprising 13 PCGs from 33 owl species and 12 PCGs from 34 species. The discrepancy in gene number resulted from the absence of the ND6 gene in the American Black-and-white Owl *Ciccaba nigrolineata*, which consequently restricted the inclusion of this species to the 12 PCGs dataset[48] (Supplementary Table S1). For partial mitochondrial analyses, the *S. ocellata* sequence was constructed from the same mitogenome employed in the COI and Cytb subset analyses. In contrast, the sequences representing other *Strix* species were retrieved from the global

GenBank repository. The COI dataset comprised 11 species represented by 48 sequences, whereas the Cytb dataset contained 12 species with 41 sequences in total (Supplementary Table S2). The phylogenetic trees were rooted using the vulnerable Great Hornbill *Buceros bicornis* (Family Bucerotidae, Order Bucerotiformes; GenBank accession number MF325011) as the outgroup[49]. All evolutionary relationships were inferred under two complementary frameworks, namely Bayesian inference (BI) and maximum likelihood (ML) approaches. For maternal phylogenetic assessment within Strigiformes, concatenated alignments of either 13 or 12 mitogenomic PCGs were generated using the concatenator module in iTaxoTools v0.1[50]. The model selection relied on the lowest Bayesian Information Criterion value, identifying the 'GTR + G + I' substitution model as the optimal evolutionary formulation for both mitogenome and partial gene datasets[51]. Notably, the BA phylogenetic inferences were performed using MrBayes v3.1.2 through the Metropolis-coupled Markov Chain Monte Carlo (MCMC) algorithm with *nst* = 6, employing one cold chain and three heated chains. The analyses proceeded for one million generations with sampling conducted every 100 generations, while the initial 25% of samples were discarded as burn-in. The convergence was assessed when the average standard deviation of split frequencies was less than or equal to 0.01, while the Potential Scale Reduction Factor approached 1 across all estimated parameters[52]. In parallel, the ML phylogenetic trees were carried out using the PhyML v3.0 web server (http://www.atgc-montpellier.fr/phyml/) under the same nucleotide substitution model[53]. All inferred trees were exported in Newick format and subsequently visualized using Interactive Tree of Life (iTOL) v7 (https://itol.embl.de/) to optimize graphical representation of tree topology[54]. Further, both intra- and interspecific genetic distances for COI and Cytb sequences within the genus *Strix* were estimated using the Kimura 2-parameter (K2P) model implemented in MEGA v12 software.

3. Results

3.1. Mitogenomic organization and structural variation

In this study, the circular mitogenome of *S. ocellata* was successfully sequenced using a sample collected from its natural habitat in India, with a total length of 19,135 bp, and was subsequently deposited in the GenBank under the accession number PX652377 (Fig. 1). The assembled mitogenome contained 37 genes, including 13 PCGs, 22 tRNA genes, two rRNA genes, and two non-coding CRs. Specifically, 30 genes were located on the heavy strand (H-strand), whereas the remaining nine genes, comprising one PCG (ND6) and eight tRNA genes, were encoded on the light strand (L-strand) (Table 1). The nucleotide composition of the *S. ocellata* mitogenome was dominated by adenine (A) at 30.67% and cytosine (C) at 32.13%, with an overall A + T content of 54.86%. The nucleotide bias examination revealed a positive AT-skew (0.118) and a negative GC-skew (− 0.424). The comparative analysis with mitogenomes of other species within the genus *Strix* indicated that genome sizes varied from 16,307 bp in *S. leptogrammica* to 19,889 bp in *S. occidentalis*. Across these species, the A + T content ranged from 52.41% to 55.59%, and the nucleotide bias pattern remained consistent, exhibiting positive AT-skew and negative GC-skew values (Table 2). Further investigation of genome organization demonstrated variations in the lengths of intergenic spacers and overlapping regions between genes in *S. ocellata*. In total, 14 intergenic spacer regions were identified with a combined length of 53 bp, along with 14 overlapping regions totaling 47 bp. The longest intergenic spacer

(13 bp) occurred between the tRNA-Leu (L2) and ND1 genes, whereas the longest overlap (10 bp) was detected in two gene pairs: between COI and tRNA-Ser (S2), and between ATP8 and ATP6. Similar overlapping patterns were also observed in other *Strix* species, with lengths ranging from 9 to 10 bp, suggesting that the mitochondrial gene organization within this genus was generally conserved despite minor variations (Supplementary Table S3).

Table 1
The organization of *S. ocellata* mitogenome, including annotated genes, their boundaries, lengths, and intergenic nucleotides.

Gene	Start	End	Strand	Size (bp)	Intergenic Nucleotide	Anti-Codon	Start Codon	Stop Codon
tRNA-Phe (F)	1	67	H	67	-2	GAA		
12S rRNA	66	1051	H	986	-2			
tRNA-Val (V)	1050	1122	H	73	1	TAC		
16S rRNA	1124	2706	H	1583	-2			
tRNA-Leu (L2)	2705	2779	H	75	13	TAA		
ND1	2793	3752	H	960	-3		ATG	AGG
tRNA-Ile (I)	3750	3822	H	73	10	GAT		
tRNA-Gln (Q)	3833	3904	L	72	-1	TTG		
tRNA-Met (M)	3904	3973	H	70	0	CAT		
ND2	3974	5014	H	1041	-3		ATG	T--
tRNA-Trp (W)	5012	5088	H	77	0	TCA		
tRNA-Ala (A)	5089	5158	L	70	0	TGC		
tRNA-Asn (N)	5159	5234	L	76	1	GTT		
tRNA-Cys (C)	5236	5305	L	70	-2	GCA		
tRNA-Tyr (Y)	5304	5377	L	74	0	GTA		
COI	5378	6929	H	1552	-10		ATG	AGG
tRNA-Ser (S2)	6920	6994	L	75	2	TGA		
tRNA-Asp (D)	6997	7066	H	70	2	GTC		
COII	7069	7752	H	684	8		ATG	TAA
tRNA-Lys (K)	7761	7829	H	69	1	TTT		

Gene	Start	End	Strand	Size (bp)	Intergenic Nucleotide	Anti-Codon	Start Codon	Stop Codon
ATP8	7831	7998	H	168	-10		ATG	TAA
ATP6	7989	8672	H	684	-1		ATG	TAA
COIII	8672	9455	H	784	-1		ATG	T--
tRNA-Gly (G)	9455	9524	H	70	0	TCC		
ND3	9525	9876	H	352	1		ATA	TAA
tRNA-Arg (R)	9878	9947	H	70	1	TCG		
ND4L	9949	10245	H	297	-7		ATG	TAA
ND4	10239	11616	H	1378	-1		ATG	T--
tRNA-His (H)	11616	11686	H	71	2	GTG		
tRNA-Ser (S1)	11689	11754	H	66	-2	GCT		
tRNA-Leu (L1)	11753	11824	H	72	0	TAG		
ND5	11825	13645	H	1821	3		ATG	TAA
Cytb	13649	14791	H	1143	0		ATG	TAA
tRNA-Thr (T)	14792	14861	H	70	0	TGT		
Control region	14862	16555	H	1694	0			
tRNA-Pro (P)	16556	16626	L	71	6	TGG		
ND6	16633	17154	L	522	2		ATG	TAG
tRNA-Glu (E)	17157	17230	L	74	0	TTC		
Control region	17231	19135	H	1905	.			

Table 2
The comparative nucleotide composition of mitogenomes across six different *Strix* species.

Species Name	GenBank Accession No.	Size (bp)	A%	T%	G%	C%	A + T%	AT-Skew	GC-Skew
Complete mitogenome									
Strix ocellata	PX652377	19,135	30.67	24.20	13.01	32.13	54.86	0.118	-0.424
Strix aluco	OP850567	18,632	29.57	23.66	14.09	32.67	53.24	0.111	-0.397
Strix leptogrammica	KC953095	16,307	29.82	22.60	14.93	32.65	52.41	0.138	-0.372
Strix occidentalis	MF431746	19,889	31.08	24.51	13.21	31.20	55.59	0.118	-0.405
Strix uralensis	MG681081	18,708	29.62	23.63	14.04	32.71	53.24	0.113	-0.399
Strix varia	MF431745	18,975	29.91	23.67	14.02	32.40	53.58	0.117	-0.396
PCGs									
Strix ocellata	PX652377	11,383	28.65	24.32	13.35	33.68	52.96	0.082	-0.432
Strix aluco	OP850567	11,382	27.47	24.50	14.34	33.68	51.98	0.057	-0.403
Strix leptogrammica	KC953095	11,420	27.74	24.02	14.12	34.12	51.76	0.072	-0.414
Strix occidentalis	MF431746	11,379	28.48	25.13	13.55	32.83	53.62	0.062	-0.416
Strix uralensis	MG681081	11,382	27.43	24.44	14.41	33.72	51.87	0.058	-0.401
Strix varia	MF431745	11,382	27.70	24.52	14.36	33.42	52.22	0.061	-0.399
tRNAs									
Strix ocellata	PX652377	1,575	28.38	27.62	22.41	21.59	56.00	0.014	0.019
Strix aluco	OP850567	1,554	32.63	23.55	17.37	26.45	56.18	0.162	-0.207
Strix leptogrammica	KC953095	1,551	33.33	23.34	17.09	26.24	56.67	0.176	-0.211
Strix occidentalis	MF431746	1,554	32.69	24.39	16.92	26.00	57.08	0.145	-0.211
Strix uralensis	MG681081	1,552	32.35	23.32	17.46	26.87	55.67	0.162	-0.212
Strix varia	MF431745	1,555	32.48	23.60	17.43	26.50	56.08	0.158	-0.206
rRNAs									
Strix ocellata	PX652377	2,569	33.13	18.92	18.72	29.23	52.04	0.273	-0.219

Species Name	GenBank Accession No.	Size (bp)	A%	T%	G%	C%	A + T%	AT-Skew	GC-Skew
Complete mitogenome									
Strix aluco	OP850567	2,559	32.79	18.37	19.15	29.70	51.15	0.282	-0.216
Strix leptogrammica	KC953095	2,571	32.28	18.44	19.53	29.75	50.72	0.273	-0.208
Strix occidentalis	MF431746	2,582	33.00	19.05	18.78	29.16	52.05	0.268	-0.216
Strix uralensis	MG681081	2,556	33.18	18.35	19.13	29.34	51.53	0.288	-0.211
Strix varia	MF431745	2,601	32.37	18.69	19.03	29.91	51.06	0.268	-0.222
CRs									
Strix ocellata	PX652377	3,599	30.73	31.79	10.78	26.70	62.52	-0.017	-0.425
Strix aluco	OP850567	1,747	27.70	29.77	13.85	28.68	57.47	-0.036	-0.349
Strix leptogrammica	KC953095	741	27.53	32.39	29.82	10.26	59.92	-0.081	0.488
Strix occidentalis	MF431746	4,340	32.83	29.56	11.98	25.62	62.39	0.052	-0.363
Strix uralensis	MG681081	3,105	29.05	29.66	12.50	28.79	58.71	-0.010	-0.395
Strix varia	MF431745	3,405	30.16	29.02	12.75	28.08	59.18	0.019	-0.376

3.2. Characteristics of protein-coding genes

The mitogenome of *S. ocellata* sequenced in this study contained 13 PCGs with a total length of 11,383 bp, representing 59.49% of the entire mitogenome. Among these genes, the shortest was ATP8 (168 bp), whereas the longest was ND5 (1,821 bp) (Table 1). The nucleotide composition of the PCGs consisted of 28.65% adenine (A), 24.32% thymine (T), 13.35% guanine (G), and 33.68% cytosine (C), which resulted in an A + T content of 52.96%. The nucleotide bias analysis also revealed an AT-skew of 0.082 and a GC-skew of − 0.432. In comparison with other species within the genus *Strix*, the total length of PCGs showed relatively limited variation. The shortest PCG length was detected in *S. occidentalis* (11,379 bp), while the longest occurred in *S. leptogrammica* (11,420 bp). Other species, including *S. aluco*, *S. uralensis*, and *S. varia*, exhibited nearly identical PCG lengths of 11,382 bp. The nucleotide composition of PCGs across the genus *Strix* also displayed a similar pattern, characterized by the predominance of adenine (A) and cytosine (C). The proportion of adenine (A) ranged from 27.43% to 28.65%, thymine (T) from 24.02% to 25.13%, guanine (G) from 13.35% to 14.41%, and cytosine (C) from 32.83% to 34.12%. Overall, the A + T content spanned from 51.76% to 53.62%, which suggested a moderate A + T compositional bias. The AT-skew values among *Strix* species varied from 0.057 to 0.082, whereas GC-skew values covered from − 0.432 to − 0.399 (Table 2). Further, the analysis of initiation and termination codons in the 13 PCGs of the *S. ocellata*

mitogenome indicated that most genes used ATG as the start codon. Only one gene, ND3, employed a different initiation codon (ATA). For termination codons, most genes utilized TAA, including ATP6, ATP8, COII, Cytb, ND3, ND4L, and ND5. Several genes encoded alternative stop codons, such as AGG in COI and ND1, as well as TAG in ND6. In addition, some genes exhibited incomplete stop codons, namely COIII, ND2, and ND4, which ended with T–. The comparison with other *Strix* species illustrated that start codon usage was relatively conserved. Most genes in *S. aluco*, *S. leptogrammica*, *S. occidentalis*, *S. uralensis*, and *S. varia* also possessed ATG as the primary start codon, with the same exception identified in ND3, which began with ATA in all species. Minor variation was confirmed in the ND5 gene, where TTG served as the start codon in *S. aluco* and *S. uralensis*, whereas the remaining species retained ATG. Conversely, the stop codons were also highly conserved among species of the genus *Strix*. Most genes terminated with TAA as the primary stop codon, although some variations were established. Notably, COII and ND6 in *S. occidentalis* adopted TAG, while Cytb, ND3, and ND6 in *S. leptogrammica* also concluded with TAG. A similar pattern was recorded in *S. varia*, which completed with TAG in ND3 and ND6, as well as in ND6 of *S. aluco*. Incomplete stop codons (T–) in COIII, ND2, and ND4 were consistently found across all analyzed species, indicating a conserved pattern within the mitogenomes of this genus. An additional variation was documented in ND5 of *S. leptogrammica*, which possessed a TA- termination codon, also representing an incomplete stop codon (Supplementary Table S4).

3.3. Nucleotide substitution trends and relative synonymous codon usage patterns

The nucleotide diversity across the PCGs was assessed using a sliding-window approach, which yielded an average nucleotide diversity (π) of 0.1248 and identified 3,220 polymorphic sites among the six *Strix* species examined in this study (Fig. 2A). The substitution saturation tests indicated no evidence of saturation for either transitions or transversions, as demonstrated by the progressive increase in Tamura–Nei (TN93) genetic distance values across the analyzed PCGs (Fig. 2B). The selective pressure was further evaluated by estimating Ka/Ks ratios for the newly sequenced *S. ocellata* together with five other *Strix* species. The calculated Ka/Ks values ranged from 0.0219 ± 0.0071 in COI to 0.5936 ± 0.0656 in ND3. Based on these estimates, the genes were ranked in ascending order of Ka/Ks values as follows: COI < COII < COIII < ND1 < ATP6 < Cytb < ND4L < ND4 < ND2 < ND6 < ND5 < ATP8 < ND3 (Fig. 2C; Supplementary Table S5). Moreover, the analyses of RSCU and amino acid composition among the *Strix* species revealed variation in synonymous codon preference, suggesting the presence of codon usage bias within the PCGs. The length of the translated sequences was relatively conserved, ranging from 3,793 to 3,806 codons per species. The RSCU profiles consistently indicated that the alanine codon GCG and the proline codon CCG were the least frequently used among their respective synonymous codons in both *S. ocellata* and the other investigated owl species. In *S. ocellata*, a total of 31 codons (48.44%) exhibited RSCU values equal to or greater than one, whereas the remaining 33 codons (51.56%) displayed RSCU values below one among the complete set of codons analyzed (Fig. 3A; Supplementary Table S6). Subsequent examination of codon usage patterns within this owl genus revealed that among the amino acids encoded by the PCGs, arginine, leucine, and serine were the most abundant residues, while methionine and tryptophan were the least represented (Fig. 3B). Focusing on *S. ocellata*, arginine, leucine, and serine accounted for 7.38%, 14.13%, and 8.75% of

the total amino acid composition, respectively, whereas methionine and tryptophan were the least constituted, contributing only 1.34% and 1.11%, respectively (Supplementary Table S7).

3.4. Configuration profiles of ribosomal and transfer RNA genes

The newly sequenced mitogenome of *S. ocellata* contained two rRNA genes (12S and 16S) with a combined length of 2,569 bp and 22 tRNA genes totaling 1,575 bp, constituting 13.42% and 8.23% of the mitogenome, respectively (Table 1). The rRNA genes of this owl species exhibited an A + T compositional bias of 52.04%, with an AT-skew of 0.273 and a GC-skew of − 0.219. The comparative analysis across available *Strix* mitogenomes indicated that total rRNA length was recorded between 2,556 bp in *S. uralensis* to 2,601 bp in *S. varia*. The A + T content of rRNAs varied from 50.72% in *S. leptogrammica* to 52.05% in *S. occidentalis*, with AT-skew values ranging from 0.268 (*S. occidentalis* and *S. varia*) to 0.288 (*S. uralensis*) as well GC-skew values from − 0.208 (*S. leptogrammica*) to − 0.222 (*S. varia*). Furthermore, the total length of tRNA genes in *S. ocellata* was slightly longer than that of other *Strix* species, which spanned from 1,551 bp in *S. leptogrammica* to 1,555 bp in *S. varia*. The tRNAs of *S. ocellata* showed a moderate A + T bias of 56.00%, comparable to other *Strix* species, which ranged from 55.67% in *S. uralensis* to 57.08% in *S. occidentalis*. The AT-skew value for tRNAs in *S. ocellata* was 0.014, lower than those observed in other congeners, and the GC-skew was positive (0.019), whereas the other five congeners displayed negative values (Table 2). In addition, the tRNA molecules of *S. ocellata* possessed conserved structural domains, including the acceptor stem, dihydrouridine (DHU) arm, anticodon loop, and TΨC arm (Supplementary Fig. S1). Notably, tRNA-Ser (S1) revealed a simplified secondary structure due to the absence of stable base pairing in the DHU arm. The predicted secondary structures were stabilized by canonical Watson–Crick base pairs (A–T and G–C) and wobble G–U interactions, each contributing 50% and providing structural flexibility while maintaining functional stability. Specifically, the G–U wobble base pairs were detected in 11 tRNAs, viz., tRNA-Ile, tRNA-Gln, tRNA-Ala, tRNA-Asn, tRNA-Cys, tRNA-Tyr, tRNA-Ser (S2), tRNA-Lys, tRNA-Leu (L1), tRNA-Pro, and tRNA-Glu (Supplementary Fig. S1).

3.5. Architectural domains and tandem repeat elements in the non-coding control region

The combined length of both CRs (CR1 + CR2) in *S. ocellata* was 3,599 bp, corresponding to 18.81% of the entire mitogenome (Table 1). This region was associated with an A + T content of 62.52%, with negative AT-skew (− 0.017) and GC-skew (− 0.425) values. The comparison of nucleotide composition in this non-coding region excluded *S. leptogrammica*, as this species possesses only a single CR of 741 bp, with an A + T content of 59.92% and AT-skew and GC-skew values of − 0.081 and 0.488, respectively. Among other *Strix* species, the CR length fluctuated from 1,747 bp in *S. aluco* to 4,340 bp in *S. occidentalis*, while the A + T content varied between 57.47% in *S. aluco* and 62.39% in *S. occidentalis*. The AT-skew values were − 0.081 in *S. leptogrammica* to 0.052 in *S. occidentalis*, whereas the GC-skew values ranged from − 0.395 in *S. uralensis* to − 0.349 in *S. aluco* (Table 2). Importantly, the present analysis demonstrated that the CRs of the five examined *Strix* species (*S. ocellata*, *S. aluco*, *S. occidentalis*, *S. uralensis*, and *S. varia*) exhibited a relatively similar structural organization, divided into three main domains (Domains I, II, and III) (Fig. 4).

Specifically, the Domain I constituted the longest region, including ETAS-1, ETAS-2, and CSB-1-like, with consensus lengths of 67, 70, and 28 bp, respectively. The Domain II encompassed multiple characteristic regulatory motifs, such as F-box (29 bp), E-box (20 bp), D-box (25 bp), C-box (29 bp), bird-similarity box (16 bp), and B-box (17 bp). The Domain III was distinguished by the presence of the CSB-1 motif, with a consensus length of 27 bp. The proportion of conserved sequences within each domain was quantified as follows: in Domain I, ETAS-1 showed 70.15%, ETAS-2 51.43%, and CSB-1-like 64.29%; in Domain II, F-box presented 86.21%, E-box 75%, D-box 88%, C-box 89.66%, bird-similarity box 93.75%, and B-box 76.47%; in Domain III, CSB-1 reached 59.26%. Further analysis revealed interspecific variation in the length of the CRs and their tandem repeats. In *S. ocellata*, the CR extended 1–144 bp in the initial segment, comprising several tandem repeats, followed by repeat blocks of 22–89 bp with variable copy numbers, and terminated at 1,880–1,905 bp. A slightly different pattern was observed in *S. aluco*, with an initial segment of 1–117 bp, tandem repeats ranging from 22–78 bp, and a terminal region at 1,518–1,549 bp. In another congener, *S. occidentalis*, the CR began at 1–108 bp and included more complex tandem repeat units (44 bp, 22 bp, 37 bp, 139 bp, 70 bp, and 78 bp) with variable copy numbers, ending at 2,284–2,319 bp. For *S. uralensis*, the initial segment spanned 1–118 bp with tandem repeats of 22 bp, 44 bp, 78 bp, 21 bp, and 156 bp, while the terminal region covered from 1,600–1,640 bp. Lastly, *S. varia* contained an initial segment of 1–127 bp with 22 bp and 78 bp tandem repeats, and a terminal block at 1,696–1,719 bp (Fig. 4).

3.6. Mitogenome-based phylogenetic placement

In the present study, the phylogenetic relationships among owls (Strigiformes) were inferred from mitogenomes using BI, with emphasis on the placement of the target species *S. ocellata* (Figs. 5A and 5B). The cladistic patterns were demonstrated based on two main datasets: 33 species with 13 PCGs (Fig. 5A) and 34 species with 12 PCGs, the latter including *C. nigrolineata*, which lacked the ND6 gene (Fig. 5B). Most nodes in the BI trees of both datasets were strongly supported by high values of posterior probability. A clear distinction emerged between the two major families, viz., Tytonidae and Strigidae. Notably, the Tytonidae formed a strongly monophyletic clade, whereas Strigidae displayed non-monophyly. Within Strigidae, the genus *Strix* constituted a monophyletic clade and presented close phylogenetic affinity to the genus *Bubo*, although *Bubo* was non-monophyletic due to the separation of *Bubo virginiatus* from the main clade. The genus Ninox also exhibited non-monophyly, whereas other genera (*Glaucidium*, *Athene*, *Otus*, and *Asio*) maintained monophyly in both datasets. More specifically, the placement of *S. ocellata* suggested a potentially basal position relative to the five other *Strix* species. Interestingly, *C. nigrolineata* appeared closely related to *S. varia* in the 12-PCG dataset, highlighting the need for further investigation to validate this relationship (Figs. 5A and 5B). Overall, the BI findings were largely consistent with ML phylogenies for both datasets, except that the genus *Glaucidium* detected non-monophyletic in the 13-PCG ML tree, while remaining monophyletic in the 12-PCG ML tree (Supplementary Figs. S2 and S3).

3.7. Gene rearrangements in Strigiformes

The mitochondrial gene arrangements of various Strigiformes species examined in this study revealed a generally conserved pattern, despite interspecific variation (Fig. 6). Specifically, the ribosomal genes 12S and 16S, 11 PCGs including COI, COII, COIII, ND1, ND2, ND3, ND4, ND4L, ND5, ATP6, and ATP8, as well as 19

tRNA genes, retained conserved positions consistent with the typical vertebrate mitogenome. Nevertheless, the mitochondrial gene rearrangements were detected in certain genes, such as two PCGs (ND6 and Cytb), three tRNAs (tRNA-Glu, tRNA-Thr, and tRNA-Pro), and the CR. Notably, 22 owl species were characterized by transpositions in ND6, Cytb, and the three aforementioned tRNAs. Additionally, three *Bubo* species (*B. virginianus*, *B. scandiacus*, and *B. bubo*) as well as five *Strix* species (*S. ocellata*, *S. varia*, *S. occidentalis*, *S. uralensis*, and *S. aluco*) displayed transpositions in ND6, Cytb, and tRNA-Glu, tRNA-Thr, and tRNA-Pro, accompanied by transposition and duplication in the CR, representing distinct gene rearrangement events. Furthermore, two other *Bubo* species (*B. flavipes* and *B. blakistoni*) exhibited a more complex mitogenome configuration, in which, in addition to the Cytb transposition, ND6, tRNA-Glu, tRNA-Thr, tRNA-Pro, and the CR underwent both transposition and duplication. Within the genus *Strix*, only *S. leptogrammica* showed a gene arrangement distinct from that of its five congeners, possessing a single CR, thereby further highlighting the occurrence of gene rearrangements in Strigiformes (Fig. 6).

3.8. Partial mtDNA-based genetic distance and phylogenetic inference of *Strix*

The mean interspecific genetic distances among *Strix* species, estimated using K2P models based on partial COI and Cytb sequences, ranged from 0.776–19.793% and 0.391–18.521%, respectively (Supplementary Tables S7 and S8). In the COI dataset, *S. ocellata* demonstrated the lowest interspecific genetic distance with *S. occidentalis* (11.264%), whereas the highest divergence was observed between *S. ocellata* and *S. leptogrammica* (19.793%) (Supplementary Table S7). Similarly, based on Cytb sequences, *S. ocellata* showed the lowest interspecific genetic distance with *S. virgata* (10.028%), while the greatest divergence was detected with *S. leptogrammica* (17.054%) (Supplementary Table S8). Furthermore, the phylogenetic analysis employing the BI and ML approaches with two mitochondrial markers (COI and Cytb) produced tree topologies that broadly illustrated the pattern of interspecific relationships within the genus *Strix*, although several differences in the relative placement of certain taxa remained evident (Figs. 7A and 7B; Supplementary Figs. S4 and S5). In the BI tree inferred from the COI gene, *S. ocellata* appeared as an early-diverging lineage relative to most other *Strix* species. This taxon occurred on a branch adjacent to several congeners (*S. occidentalis*, *S. hylophila*, *S. rufipes*, *S. virgata*, and *S. varia*, which together formed a clade supported by relatively strong posterior probability (Fig. 7A). In contrast, the BI phylogeny derived from the Cytb gene also retained *S. ocellata* as an early lineage within the genus *Strix*, yet displayed a slightly different pattern of relationships compared with the COI result. Under this phenomenon, *S. ocellata* associated with another assemblage of *Strix* species arranged in a distinct clade with varying levels of posterior support (Fig. 7B). Within the ML framework, the general pattern in which *S. ocellata* represented an early-diverging lineage in *Strix* was consistent, although its closest affinities differed depending on the genetic marker analyzed. In the COI construction, *S. ocellata* occupied a branch proximal to *S. leptogrammica*. This relationship was distinct from another clade including five additional *Strix* species (*S. occidentalis*, *S. hylophila*, *S. rufipes*, *S. virgata*, and *S. varia*) (Supplementary Fig. S4). Conversely, the Cytb gene in ML tree indicated a closer association between *S. ocellata* and four other species (*S. occidentalis*, *S. virgata*, *S. rufipes*, and *S. varia*). In the same construction, *S. leptogrammica* constituted a separate clade with affinity to a lineage comprising *Strix omanensis*, *Strix butleri*, and *Strix hadorami* (Supplementary Fig.

S5). These three species remained absent from the COI dataset in both BI and ML because sequences of this gene were unavailable in the global GenBank repository. Nevertheless, a single Cytb sequence of *S. hadorami* in both BI and ML occupied a position within the *S. butleri* clade, thereby requiring further validation to confirm the accuracy of its placement (Figs. 7A and 7B; Supplementary Figs. S4 and S5). In a subsequent clade, across the Cytb BI tree as well as the COI and Cytb ML analyses, *Strix woodfordii* represented an isolated branch preceding a larger assemblage containing *S. aluco* and *S. uralensis*. These two species comprised a large clade with a relatively high number of sequence samples (Fig. 7B; Supplementary Figs. S4 and S5). However, in the COI BI tree, *S. woodfordii* clustered near *S. leptogrammica*, where both taxa exhibited a polytomous relationship (Fig. 7A). Additionally, a single sequence of *Strix davidi* in the COI topology of both BI and ML was found near—and even within—the *S. uralensis* clade, a pattern that necessitated further examination to verify this position (Figs. 7A; Supplementary Fig S4).

4. Discussion

4.1. Comparative mitogenomic insights into *Strix* species

Generating complete mitogenomes in owls provides significant value, as it offers comprehensive genetic data relevant for taxonomic, phylogenetic, and conservation studies, particularly within the *Strix* lineage[23–25]. Accordingly, the present study expands the existing molecular dataset by presenting the complete mitogenome of morphologically identified as *S. ocellata* for the first time. The mitogenomic analysis reveals that this species possesses a circular genome comprising 37 genes and two CRs. The gene distribution across the heavy and light strands follows the functional patterns typical of extant birds and aligns with other *Strix* species[23–25]. The presence of double CRs in *S. ocellata* corresponds with prior observations in birds, where one or two CRs are generally reported[23,25,55]. The initiation and termination codon analyses in *Strix* species demonstrate that most genes utilize the ATG initiation codon, with the exception of ND3, which employs ATA as an alternative, a feature commonly found in modern birds[56]. The TAA stop codon is conserved and predominant, whereas TAG, AGG, and incomplete stop codons (T–/TA-) occur as minor variants, reflecting mitochondrial translational flexibility in aves[55]. Moreover, the incomplete stop codons observed among *Strix* taxa are likely extended post-transcriptionally through polyadenylation[57]. The selection analyses of PCGs in the genus *Strix* indicate Ka/Ks ratios below 1, suggesting purifying selection pressure[58]. This pattern implies that potentially deleterious mutations are selectively eliminated, thereby maintaining essential gene functions critical for adaptation and survival of this *Strix* lineage[59,60]. Among them, the COI emerges as the most conserved gene, supporting its potential as a barcoding marker for *Strix* species, consistent with selection studies in other owls[58]. Leucine, serine, and arginine are more frequently represented among *Strix* taxa due to their multiple synonymous codons, while methionine and tryptophan are comparatively rare, reflecting a typical codon usage bias in birds that may be shaped by mutational pressure, translational selection, and genomic guanine-cytosine composition[61]. Additionally, the simplified secondary structure of tRNA-Ser (S1) detected in this study, characterized by the absence of a stable DHU arm, is a highly conserved feature in vertebrate mitogenomes, including those of birds[62].

Furthermore, the comparative examination of CRs across the five investigated *Strix* species (*S. ocellata*, *S. varia*, *S. occidentalis*, *S. uralensis*, and *S. aluco*) shows that all possess two CRs, whereas *C. leptogrammica* exhibits only one. Functionally, the *Strix* mitogenomes with two CRs enable simultaneous replication initiation at both CRs, thereby accelerating replication relative to single-CR mitogenomes[55,63]. Double CRs are also thought to support efficient replication and transcription of multiple loci simultaneously, thus supplying the cellular energy demands in these birds[64]. Interestingly, the CR structure in these five *Strix* species divides into three domains, reflecting patterns consistent with other species of Strigiformes[46]. Specifically, Domain I containing ETAS participates in termination of heavy-strand replication, Domain II likely regulates heavy-strand synthesis, with B-box, D-box, and F-box predominating over C-box and E-box, as well as Domain III, encompassing CSB-1, mediates mitogenome replication and transcription initiation[46]. The tandem repeat evaluation detects interspecific variation in repeat length and unit number among *Strix* species, confirming the dynamic evolution of CRs within this lineage[46,65,66]. Remarkably, the previous hypotheses also suggest that accumulation of tandem repeats in vertebrates may correlate with individual age, potentially influencing mitochondrial function and aging[66]. While the current study does not directly address this issue, future temporal analyses using different tissue samples (such as blood or feathers) from *S. ocellata* and other bird species may help explain the development of tandem repeat variation and its effects on mitochondrial function. Importantly, the major mitochondrial gene arrangement (12S, 16S, 11 PCGs, and 19 tRNAs) remains relatively conserved across all observed owls, confirming the stability of the basic mitogenome structure. However, certain genes and CR in multiple *Strix* and *Bubo* species undergo transpositions and duplications, indicating genetic rearrangement as a principal evolutionary mechanism driving mitogenomic variation in owls[23,24].

4.2. Matrilineal phylogenetic inference and biogeographic interpretation

Understanding phylogenetic relationships among bird species constitutes a fundamental aspect of evolutionary biology, serving not only as a record of speciation history but also as a foundation for comparative analyses of species traits, including owls[67]. In line with this framework, the present study constructs a matrilineal phylogeny of the order Strigiformes, revealing that Strigidae is non-monophyletic at the family level, while Tytonidae forms a well-supported monophyletic clade. These findings align with previous work highlighting the evolutionary complexity within Strigidae, where numerous genera display paraphyletic or polyphyletic arrangements based on nuclear gene analyses[13]. Conversely, the Tytonidae corroborates the hypothesis of family-level monophyly and supports a sister-group relationship between the genera *Tyto* and *Phodilus*, as evidenced by partial mito-nuclear loci[7,14]. Within Strigidae, the analyses of complete mitogenomes and two partial mitochondrial datasets (COI and Cytb) uncover novel insights, particularly the potential basal placement of *S. ocellata* among the *Strix* species examined. Moreover, the genus *Strix* establishes a monophyletic clade and exhibits close affinity with the genus *Bubo*, consistent with prior observations derived from mitogenomes, partial mitochondrial sequences, and nuclear genes[7,24,25]. From a biogeographical perspective, these genera demonstrate overlapping distributions, with *Bubo* spanning the Americas, the Arabian Peninsula, the Indian subcontinent, and Africa, potentially enhancing ecological interactions among species[6]. The outcomes of this study further correspond to

mitogenome-based phylogenies positioning the clade *Otus* + *Asio* + *Bubo* + *Strix*, indicating that *Otus* diverged earlier than the remaining three genera[24]. Moreover, the genus *Ninox* shows non-monophyly, while *C. nigrolineata* aligns closely with *S. varia*, consistent with previous mitogenomic studies[25]. Four additional genera within Strigidae (*Glaucidium*, *Athene*, *Otus*, and *Asio*) also demonstrate monophyly, corroborating prior data from mitogenomes, partial mitochondrial sequences, and nuclear genes[7,25]. The observed non-monophyly and intricate relationships within Strigidae underscore the necessity for broad taxonomic sampling, further comprehensive investigations, and potential taxonomic revisions[13]. Focusing on the partial COI sequences in the ML tree within *Strix*, the *S. ocellata* is closely with *S. leptogrammica*, consistent with the topology recovered from the larger mitogenome dataset. In a biogeographic context, *S. leptogrammica* displays a broad distribution, encompassing South Asia, East Asia, and both the mainland and islands of Southeast Asia, with some of its range overlapping with *S. ocellata*[68]. Additionally, a sequence of *S. davidi* within the COI tree appears adjacent to—or even nested within—the *S. uralensis* clade, supporting prior findings that *S. davidi* represents one of eleven *S. uralensis* subspecies with a natural distribution in China, suggesting this placement is plausible[6,69].

Conclusion

This study characterized the complete mitogenome of *S. ocellata* (19,135 bp), comprising the standard set of 37 mitochondrial genes and two CRs. The codon usage patterns largely matched those reported for other *Strix* species, whereas the Ka/Ks analyses indicated purifying selection acting on all PCGs. The CR contained conserved domains and tandem repeat variation potentially contributing to interspecific genome length differences. The phylogenetic analyses based on mitogenomes resolved a clear separation between the families Strigidae and Tytonidae. Within Strigidae, *Strix* formed a monophyletic clade closely related to *Bubo*, while *S. ocellata* occupied a relatively basal position within the genus under the current dataset, suggesting early divergence. The analyses using partial mitochondrial genes largely supported this placement, although minor differences appeared between the COI and Cytb datasets. Overall, this study expands the mitogenomic dataset for the genus *Strix* and provides a molecular basis for investigating phylogenetic relationships, evolutionary dynamics, and future phylogeographic and conservation research on owls. Nevertheless, the current mitogenome-based dataset represents only ~ 13% of the 254 currently recognized Strigiformes species, with six of the 22 known *Strix* species included in the analysis. In contrast, partial gene datasets offered broader taxonomic representation, encompassing 11 species in the COI dataset and 12 species in the Cytb dataset (~ 50.0–54.6% of all *Strix* species), thereby providing a more representative preliminary overview of phylogenetic relationships within the genus. Thus, future studies should increase the availability of complete mitogenomes across additional species to improve phylogenetic resolution and strengthen reconstruction of the evolutionary history of this owl lineage. Apart from the global significance, this study reveals baseline information on *S. ocellata* from its Indian geographic range, as the species is known to exhibit certain morphological variations across different geographic regions within the country. Furthermore, the molecular data generated from the present study may be valuable for understanding the possible genetic variations throughout its distribution range in India.

Declarations

Data availability

The complete mitochondrial genome of *S. ocellata* generated in this study has been deposited in the GenBank database (https://www.ncbi.nlm.nih.gov/) under accession number PX652377. Please contact the corresponding authors (A.M. and S.K.) for any data requests related to this study.

Acknowledgements

The authors sincerely thank the Director of the Zoological Survey of India for providing essential facilities and institutional support to accomplish this work. The authors also express their gratitude to the staff of the Birds Section, ZSI, for their assistance during this study. The author (A.P.) acknowledge the Interdisciplinary Program of Marine and Fisheries Sciences and Convergent Technology at Pukyong National University, Busan, Republic of Korea for academic support during Ph.D. program.

Author contributions

Conceptualization: A.M., S.K; data curation: A.M., A.P., A.N., A.M.H; formal analysis: A.M., A.P., A.N., A.M.H; funding acquisition: A.M., D.B; investigation: A.M., S.K., H.W.K; methodology: A.M., A.P., A.N., A.M.H; project administration: A.M., S.K; resources: A.M., S.K; software: A.P., A.M.H., H.W.K; supervision: A.M., S.K; validation: A.P., D.B., H.W.K; visualization: A.M., A.P., D.B., S.K; writing – original draft: A.M., A.P., A.N., A.M.H; writing – review and editing: D.B., H.W.K., S.K.

Funding

This research was supported by core funding of the Zoological Survey of India, under the Ministry of Environment, Forest and Climate Change, Government of India.

Competing interests

The authors report no financial or personal conflicts of interest that could have affected the outcomes of this study.

Ethical approval

No ethical statement was reported.

Additional information

Supplementary Information

The online version contains supplementary material available at:

References

1. Miller, C. V. & Pittman, M. The diet of early birds based on modern and fossil evidence and a new framework for its reconstruction. *Biol. Rev.* **96**, 2058–2112 (2021).

2. Lees, A. C. et al. State of the World's Birds. *Annu. Rev. Environ. Resour.* **47**, 231–260 (2022).
3. Brusatte, S. L., O'Connor, J. K. & Jarvis, E. D. The origin and diversification of birds. *Curr. Biol.* **25**, R888–R898 (2015).
4. Machac, A. The dynamics of bird diversity in the New World. *Syst. Biol.* **69**, 1180–1199 (2020).
5. Horn, S. et al. Impact of birds on intertidal food webs assessed with ecological network analysis. *Estuar. Coast Shelf Sci.* **219**, 107–119 (2019).
6. Gill, F., Donsker, D. & Rasmussen, P. (eds). IOC World Bird List (v15.1). March (2026). Available at https://www.worldbirdnames.org/ (accessed 1 (2025).
7. Wink, M., El-Sayed, A. A., Sauer-Gürth, H. & Gonzalez, J. Molecular phylogeny of owls (Strigiformes) inferred from DNA sequences of the mitochondrial cytochrome b and the nuclear RAG-1 gene. *Ardea* **97**, 581–591 (2009).
8. Buechley, E. R. et al. Global raptor research and conservation priorities: Tropical raptors fall prey to knowledge gaps. *Divers. Distrib.* **25**, 856–869 (2019).
9. Smith, N. A., Stidham, T. A. & Mitchell, J. S. The first fossil owl (Aves, Strigiformes) from the Paleogene of Africa. *Diversity* **12**, 163 (2020).
10. Li, Z. et al. Early evolution of diurnal habits in owls (Aves, Strigiformes) documented by a new and exquisitely preserved Miocene owl fossil from China. *Proc. Natl Acad. Sci. U.S.A*. 119, e2119217119 (2022).
11. Cho, Y. S. et al. Raptor genomes reveal evolutionary signatures of predatory and nocturnal lifestyles. *Genome Biol.* **20**, 181 (2019).
12. McClure, C. J. W. et al. Commentary: Defining raptors and birds of prey. *J. Raptor Res.* **53**, 419–430 (2019).
13. Salter, J. F. et al. Extensive paraphyly in the typical owl family (Strigidae). *Auk* **137**, ukz070 (2020).
14. Uva, V., Päckert, M., Cibois, A., Fumagalli, L. & Roulin, A. Comprehensive molecular phylogeny of barn owls and relatives (Family: Tytonidae), and their six major Pleistocene radiations. *Mol. Phylogenet Evol.* **125**, 127–137 (2018).
15. Jackett, N. A. et al. Uncovering the calls of data-deficient masked owls using morphology and environmental gradients. *J. Biogeogr.* **52**, e70110 (2025).
16. Bontzorlos, V. A., Johnson, D. H., Poirazidis, K. & Roulin, A. Owl symbolism in Greek civilization over the last 5000 years: Social perceptions and implications for conservation. *Eur. Zool. J.* **90**, 691–707 (2023).
17. Formoso, A. E., Plaza, P. & Lambertucci, S. A. Global assessment of ecosystem services and disservices associated with owls. *Ecosyst. Serv.* **72**, 101707 (2025).
18. BirdLife International. Strix ocellata. The IUCN Red List of Threatened Species 2024: e.T22689066A263957499. (2024).
19. Pande, S. et al. Breeding biology of the mottled wood-owl (*Strix ocellata*) in west-central India. *J. Raptor Res.* **52**, 240–244 (2018).
20. Funk, W. C., Mullins, T. D., Forsman, E. D. & Haig, S. M. Microsatellite loci for distinguishing spotted owls (*Strix occidentalis*), barred owls (*Strix varia*), and their hybrids. *Mol. Ecol. Notes*. **7**, 284–286 (2007).

21. Hull, J. M. et al. Range-wide genetic differentiation among North American great gray owls (*Strix nebulosa*) reveals a distinct lineage restricted to the Sierra Nevada, California. *Mol. Phylogenet Evol.* **56**, 212–221 (2010).
22. Liu, G., Zhou, L. & Gu, C. The complete mitochondrial genome of brown wood owl *Strix leptogrammica* (Strigiformes: Strigidae). *Mitochondrial DNA A*. **25**, 370–371 (2014).
23. Hanna, Z. R. et al. Complete mitochondrial genome sequences of the northern spotted owl (*Strix occidentalis caurina*) and the barred owl (*Strix varia*; Aves: Strigiformes: Strigidae) confirm the presence of a duplicated control region. *PeerJ* **5**, e3901 (2017).
24. Kang, H., Li, B., Ma, X. & Xu, Y. Evolutionary progression of mitochondrial gene rearrangements and phylogenetic relationships in Strigidae (Strigiformes). *Gene* **674**, 8–14 (2018).
25. Wang, Y., Zhan, H., Zhang, Y., Long, Z. & Yang, X. Mitochondrial genome analysis, phylogeny, and divergence time evaluation of *Strix aluco* (Aves, Strigiformes, Strigidae). *Biodivers. Data J.* **11**, e101942 (2023).
26. Zardoya, R. Recent advances in understanding mitochondrial genome diversity. *F1000Res*. 9, F1000 Faculty Rev-270 (2020).
27. Kundu, S., Alam, I., Maheswaran, G., Tyagi, K. & Kumar, V. Complete mitochondrial genome of Great Frigatebird (*Fregata minor*): Phylogenetic position and gene rearrangement. *Biochem. Genet.* **60**, 1177–1188 (2022).
28. Xing, B., Lin, L. & Wu, Q. Application of mitochondrial genomes to species identification and evolution. *Electron. J. Biotechnol.* **76**, 39–48 (2025).
29. Jiang, C. et al. Comparative mitogenomics, phylogeny, and biogeography of selected species of *Saxicola* (Aves, Passeriformes). *ZooKeys* **1249**, 69–92 (2025).
30. Montaña-Lozano, P. et al. Comparative genomic analysis of vertebrate mitochondrial genomes reveals a differential rate of rearrangements among taxonomic classes. *Sci. Rep.* **12**, 5479 (2022).
31. Lesson, R. P. Revue Zoologique, par la Société Cuvierienne. *Rev Zool* **2**, 289 (1839).
32. Percie du Sert. The ARRIVE guidelines 2.0: Updated guidelines for reporting animal research. *PLoS Biol.* **18**, e3000410 (2020).
33. Ahmad, S., Ghosh, A., Nair, D. L. & Seshadri, M. Simultaneous extraction of nuclear and mitochondrial DNA from human blood. *Genes Genet. Syst.* **82**, 429–432 (2007).
34. Kearse, M. et al. Geneious Basic: An integrated and extendable desktop software platform for the organization and analysis of sequence data. *Bioinformatics* **28**, 1647–1649 (2012).
35. Al Arab, M. et al. Accurate annotation of protein-coding genes in mitochondrial genomes. *Mol. Phylogenet Evol.* **106**, 209–216 (2017).
36. Donath, A. et al. Improved annotation of protein-coding gene boundaries in metazoan mitochondrial genomes. *Nucleic Acids Res.* **47**, 10543–10552 (2019).
37. Iwasaki, W. et al. MitoFish and MitoAnnotator: A mitochondrial genome database of fish with an accurate and automatic annotation pipeline. *Mol. Biol. Evol.* **30**, 2531–2540 (2013).

38. Zhu, T. et al. MitoAnnotator, and MiFish Pipeline: Updates in 10 years. *Mol. Biol. Evol.* **40**, msad035 (2023).
39. Sayers, E. W. et al. Database resources of the National Center for Biotechnology Information in 2026. *Nucleic Acids Res.* **54**, D20–D27 (2026).
40. Perna, N. T. & Kocher, T. D. Patterns of nucleotide composition at fourfold degenerate sites of animal mitochondrial genomes. *J. Mol. Evol.* **41**, 353–358 (1995).
41. Kumar, S. et al. MEGA12: Molecular Evolutionary Genetic Analysis version 12 for adaptive and green computing. *Mol. Biol. Evol.* **41**, msae263 (2024).
42. Rozas, J. et al. DnaSP 6: DNA sequence polymorphism analysis of large datasets. *Mol. Biol. Evol.* **34**, 3299–3302 (2017).
43. Xia, X. DAMBE6: new tools for microbial genomics, phylogenetics, and molecular evolution. *J. Hered*. **108**, 431–437 (2017).
44. Laslett, D. & Canbäck, B. ARAGORN, a program to detect tRNA genes and tmRNA genes in nucleotide sequences. *Nucleic Acids Res.* **32**, 11–16 (2004).
45. Thompson, J. D., Higgins, D. G. & Gibson, T. J. CLUSTAL W: Improving the sensitivity of progressive multiple sequence alignment through sequence weighting, position-specific gap penalties, and weight matrix choice. *Nucleic Acids Res.* **22**, 4673–4680 (1994).
46. Xiao, B., Ma, F., Sun, Y. & Li, Q. Comparative analysis of complete mitochondrial DNA control region of four species of Strigiformes. *Acta Genet. Sin*. **33**, 965–974 (2006).
47. Benson, G. Tandem repeats finder: a program to analyze DNA sequences. *Nucleic Acids Res.* **27**, 573–580 (1999).
48. Feng, S. et al. Dense sampling of bird diversity increases power of comparative genomics. *Nature* **587**, 252–257 (2020).
49. Chen, Y., Li, C., Yan, H., Xiao, H. & Chen, S. The complete mitochondrial genome sequence of *Buceros bicornis* (Bucerotiformes: Bucerotidae). *Conserv. Genet. Resour.* **10**, 287–290 (2018).
50. Vences, M. et al. iTaxoTools 0.1: Kickstarting a specimen-based software toolkit for taxonomists. *Megataxa* **6**, 77–92 (2021).
51. Lefort, V., Longueville, J. E. & Gascuel, O. S. M. S. Smart Model Selection in PhyML. *Mol. Biol. Evol.* **34**, 2422–2424 (2017).
52. Ronquist, F. et al. MrBayes 3.2: Efficient Bayesian phylogenetic inference and model choice across a large model space. *Syst. Biol.* **61**, 539–542 (2012).
53. Guindon, S. et al. New algorithms and methods to estimate maximum-likelihood phylogenies: Assessing the performance of PhyML 3.0. *Syst. Biol.* **59**, 307–321 (2010).
54. Letunic, I. & Bork, P. Interactive Tree of Life (iTOL) v6: Recent updates to the phylogenetic tree display and annotation tool. *Nucleic Acids Res.* **52**, W78–W82 (2024).
55. Dai, C. & Lei, F. Mitogenomic variation in the Black-throated Tit (*Aegithalos concinnus*): Conserved structure, concerted evolution of duplicate control regions and multiple distinct evolutionary lineages. *Avian Res.* **15**, 100210 (2024).

56. Pacheco, M. A. et al. Evolution of modern birds revealed by mitogenomics: Timing the radiation and origin of major orders. *Mol. Biol. Evol.* **28**, 1927–1942 (2011).
57. Ojala, D., Montoya, J. & Attardi, G. tRNA punctuation model of RNA processing in human mitochondria. *Nature* **290**, 470–474 (1981).
58. Yu, J. et al. Characterization of the complete mitochondrial genome of *Otus lettia*: Exploring the mitochondrial evolution and phylogeny of owls (Strigiformes). *Mitochondrial DNA B*. **6**, 3443–3451 (2021).
59. Johnson, K. P. & Seger, J. Elevated rates of nonsynonymous substitution in island birds. *Mol. Biol. Evol.* **18**, 874–881 (2001).
60. Wirthlin, M. et al. Parrot genomes and the evolution of heightened longevity and cognition. *Curr. Biol.* **28**, 4001–4008e7 (2018).
61. Rao, Y. et al. Mutation bias is the driving force of codon usage in the *Gallus gallus* genome. *DNA Res.* **18**, 499–512 (2011).
62. Watanabe, Y., Suematsu, T. & Ohtsuki, T. Losing the stem-loop structure from metazoan mitochondrial tRNAs and co-evolution of interacting factors. *Front. Genet.* **5**, 109 (2014).
63. Shao, R., Barker, S. C., Mitani, H., Aoki, Y. & Fukunaga, M. Evolution of duplicate control regions in the mitochondrial genomes of metazoa: A case study with Australasian *Ixodes* ticks. *Mol. Biol. Evol.* **22**, 620–629 (2005).
64. Eberhard, J. R. & Wright, T. F. Rearrangement and evolution of mitochondrial genomes in parrots. *Mol. Phylogenet Evol.* **94**, 34–46 (2016).
65. Wang, X. et al. Extreme variation in patterns of tandem repeats in mitochondrial control region of yellow-browed tits (*Sylviparus modestus*, Paridae). *Sci. Rep.* **5**, 13227 (2015).
66. Serrano, M. J., Goudet, J. & Cumer, T. Characterization of the diversity of barn owl's mitochondrial genome reveals high copy number variations in the control region. *PLoS One*. **19**, e0295595 (2024).
67. Stiller, J. et al. Complexity of avian evolution revealed by family-level genomes. *Nature* **629**, 851–860 (2024).
68. BirdLife International. Strix leptogrammica. The IUCN Red List of Threatened Species 2024: e.T22689071A263957894. (2024).
69. Scherzinger, W., Fang, Y. & Sun, Y. H. The Sichuan Wood Owl *Strix uralensis davidi* from the mountain forests of China/Tibet — no longer a 'phantom'. *Ardea* **97**, 648 (2009).

Figures

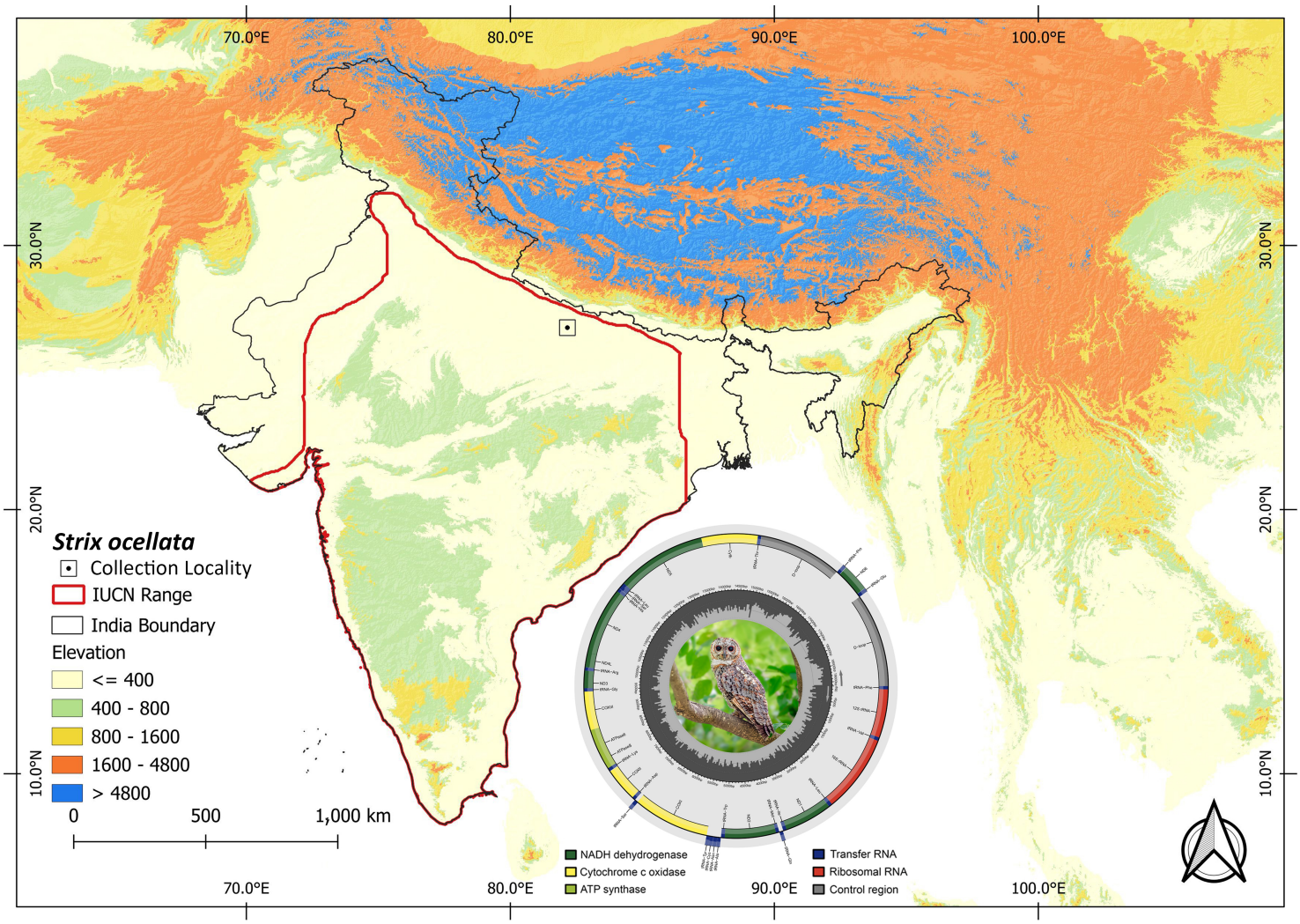


Figure 1

The biogeographic distribution of *S. ocellata*based on the IUCN Red List of Threatened Species. The red line delineates the species distribution range, while the boxed area with a central point indicates the locality where the road-kill specimen was collected. The circular diagram represents the mitogenome architecture of *S. ocellata*, generated using the MitoAnnotator web server (https://mitofish.aori.u-tokyo.ac.jp/annotation/input/). The genes are displayed with distinct color codes to facilitate structural interpretation. The distribution map was produced using ArcGIS v10.6. The species photograph was taken by the author (A.M.) and subsequently edited using Adobe Photoshop CS 8.0.

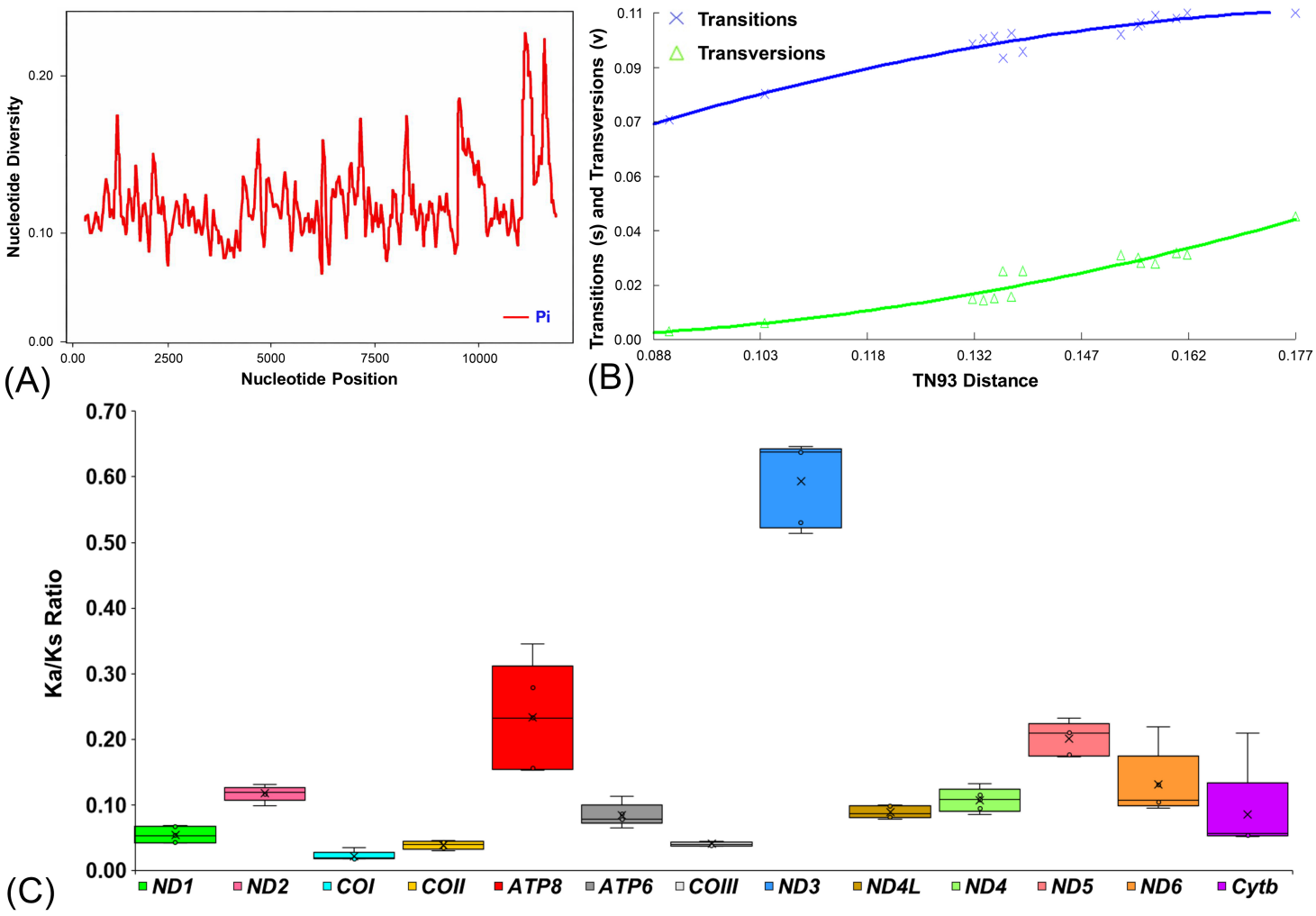


Figure 2

(A) The patterns of nucleotide diversity (π) across the 13 PCGs among representative *Strix* species. (B) The relationship between transition–transversion substitution patterns and genetic divergence estimated using Tamura–Nei (TN93) distance metrics. (C) The comparative analysis of Ka/Ks ratios across the 13 PCGs of *S. ocellata* and its related congeners. All plots were created by using Microsoft Excel v2016 and edited manually in Adobe Photoshop CS 8.0.

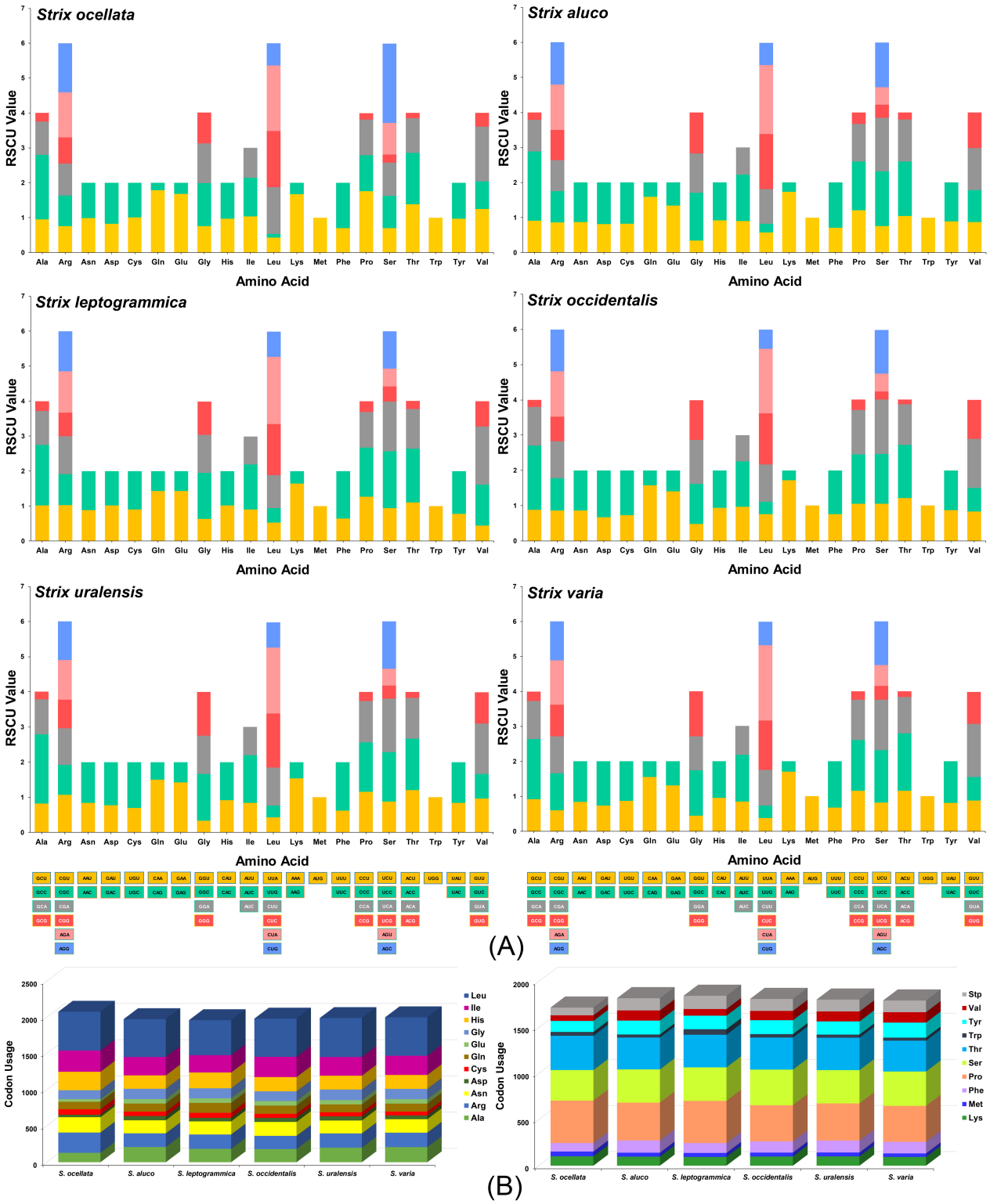


Figure 3

The structural and compositional characteristics of amino acids encoded by the 13 PCGs across six *Strix* species. (A) The RSCU profiles illustrating codon preference and translational bias for individual amino acids. (B) The comparative distribution of amino acid composition among the examined *Strix* taxa. The bar plots were developed by using Microsoft Excel v2016 and edited manually in Adobe Photoshop CS 8.0.

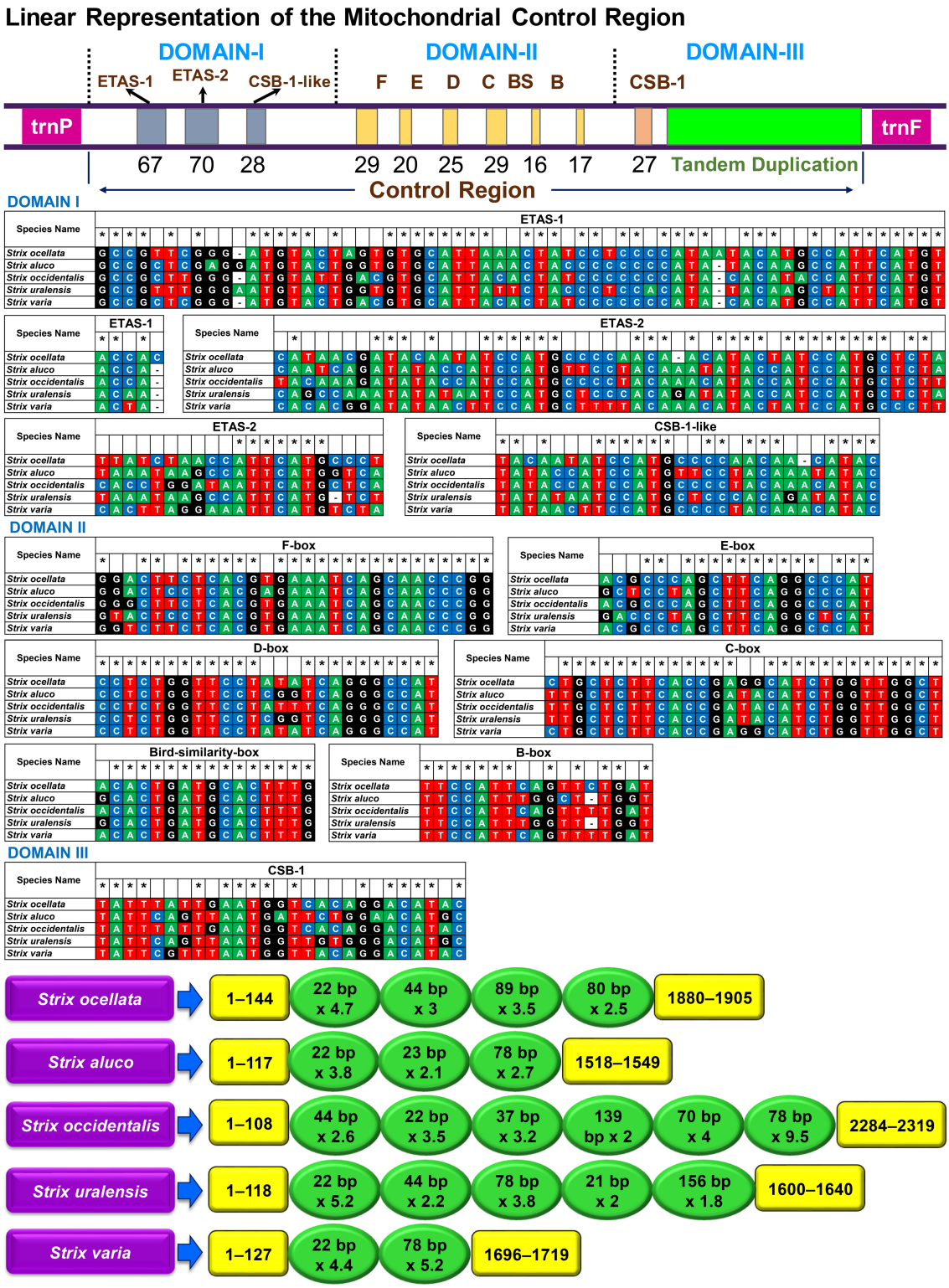


Figure 4

The linearized representation and comparative analysis of the CRs in five studied *Strix* species, illustrating the structural organization of the three principal domains and their specific elements. The upper panel depicts the general structural features of the avian CR as described in a previous study[46]. The conserved nucleotides shared among all analyzed species are indicated by star symbols across the different domains.

The species-specific variable number tandem repeat (VNTR) motifs within the CR are illustrated as green ovals, representing repeat units and their copy number variations.

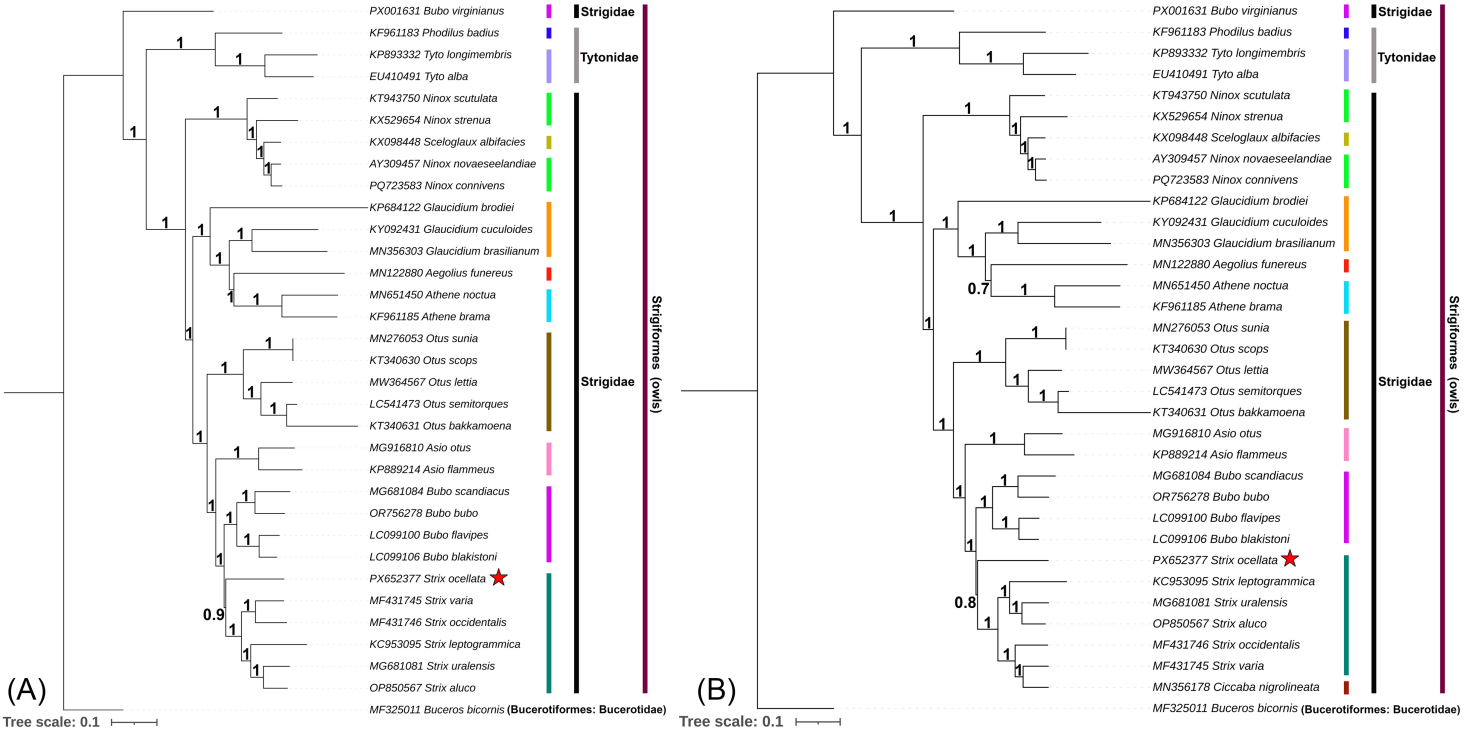


Figure 5

The BI phylogenetic trees constructed from two datasets of concatenated PCGs: (A) 33 species of Strigiformes, excluding *C. nigrolineata*, which lacks ND6 gene and (B) 34 species of Strigiformes. The BI topology demonstrates the monophyletic relationships among six *Strix* species and clearly distinguishes *S. ocellata* (red star) from other owl species in both datasets. The cladistic pattern further provides insights into evolutionary relationships across different taxonomic levels (genus and family) within the order. The BI posterior probability support values are indicated at each node (black numbers), representing the statistical support for each topology branch.

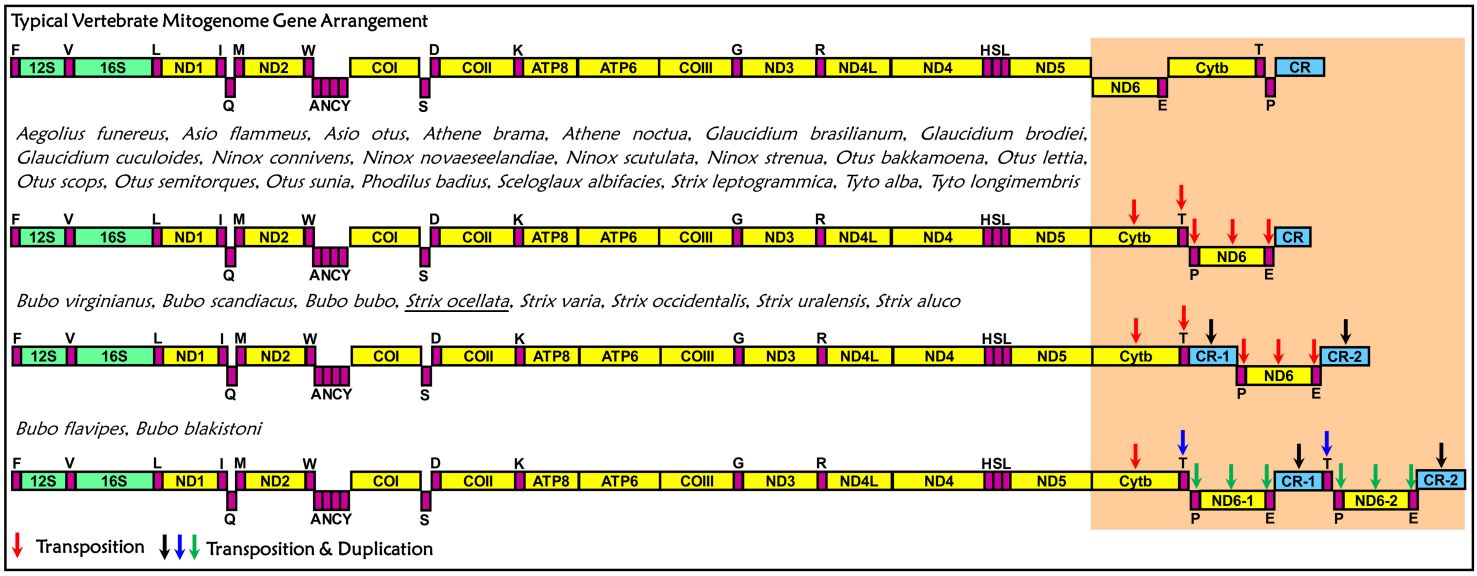


Figure 6

The comparative mitogenomic gene arrangements among representative owl species, with the typical vertebrate gene order shown at the top as a reference. The gene arrangements patterns are illustrated by differently colored boxes representing PCGs, tRNAs, rRNAs, and the CR, with the gene abbreviations. The gene variations, including transpositions and transpositions accompanied by duplication events, are denoted by different arrow symbols. Specifically, red arrows indicate transposition events, whereas black, blue, and green arrows represent transpositions associated with duplication events. The highlighted orange region represents rearrangements involving the two PCGs (Cytb and ND6), three tRNAs (E, T, P), and the CR across different taxa.

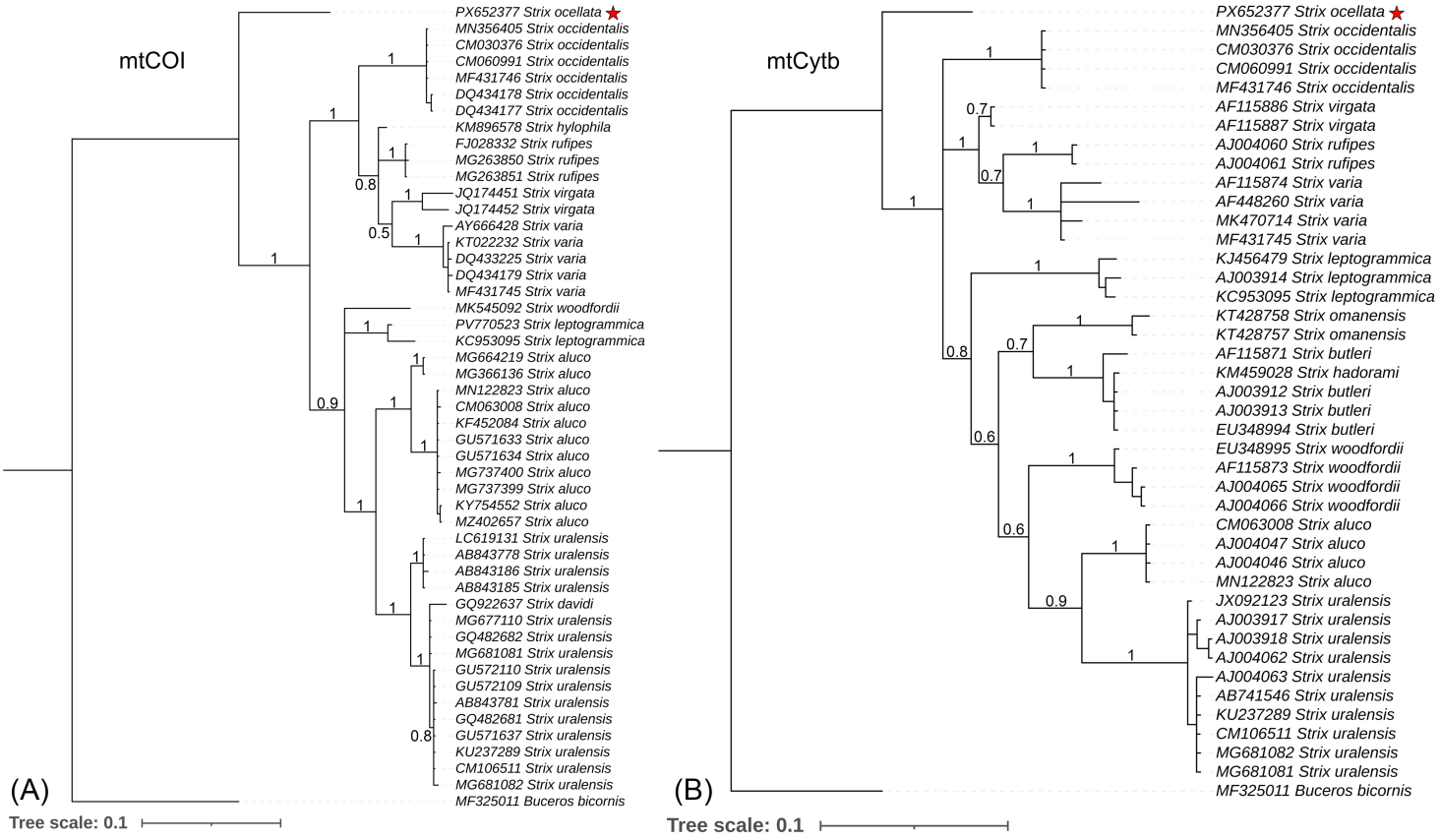


Figure 7

The BI phylogenetic trees constructed by two partial mitochondrial DNA datasets for *Strix*lineages. (A) The COI dataset comprising 11 species and (B) the Cytb dataset containing 12 species. The BI topology clearly distinguishes *S. ocellata* (red star) from other *Strix* species in both datasets. The posterior probability support values are indicated at each node (black numbers), denoting the statistical support for each branch.

Supplementary Files

This is a list of supplementary files associated with this preprint. Click to download.

- SupplementaryInformation.docx